## Advanced Virgo

T. Accadia[1], F. Acernese[2ac], P. Astone[3a], G. Ballardin[4], F. Barone[2ac], M. Barsuglia[5], A. Basti[6ab], Th. S. Bauer[7a], M. Bebronne[1], M. Bejger[8c], M.G. Beker[7a], A. Belletoile[1], M. Bitossi[6a], M. A. Bizouard[9a], M. Blom[7a], F. Bondu[10b], L. Bonelli[6ab], R. Bonnand[11], V. Boschi[6a], L. Bosi[12a], B. Bouhou[5], S. Braccini[6a], C. Bradaschia[6a], M. Branchesi[13ab], T. Briant[14], A. Brillet[10a], V. Brisson[9a], T. Bulik[8b], H. J. Bulten[7ab], D. Buskulic[1], C. Buy[5], G. Cagnoli[13a], E. Calloni[2ab], B. Canuel[4], F. Carbognani[4], F. Cavalier[9a], R. Cavalieri[4], G. Cella[6a], E. Cesarini[13b], O. Chaibi[10a], E. Chassande-Mottin[5], A. Chincarini[15], A. Chiummo[4], F. Cleva[10a], E. Coccia[16ab], P.-F. Cohadon[14], C. N. Colacino[6ab], J. Colas[4], A. Colla[3ab], M. Colombini[3b], A. Conte[3ab], J.-P. Coulon[10a], E. Cuoco[4], S. D'Antonio[16a], V. Dattilo[4], M. Davier[9a], R. Day[4], R. De Rosa[2ab], G. Debreczeni[17], W. Del Pozzo[7a], M. del Prete[18b], L. Di Fiore[2a], A. Di Lieto[6ab], M. Di Paolo Emilio[16ac], A. Di Virgilio[6a], A. Dietz[1], M. Drago[18ab], G. Endrőczi[17], V. Fafone[16ab], I. Ferrante[6ab], F. Fidecaro[6ab], I. Fiori[4], R. Flaminio[11], L. A. Forte[2a], J.-D. Fournier[10a], J. Franc[11], S. Frasca[3ab], F. Frasconi[6a], M. Galimberti[11], L. Gammaitoni[12ab], F. Garufi[2ab], M. E. Gáspár[17], G. Gemme[15], E. Genin[4], A. Gennai[6a], A. Giazotto[6a], R. Gouaty[1], M. Granata[5], C. Greverie[10a], G. M. Guidi[13ab], J.-F. Hayau[10b], A. Heidmann[14], H. Heitmann[10], P. Hello[9a], P. Jaranowski[8d], I. Kowalska[8b], A. Królak[8ae], N. Leroy[9a], N. Letendre[1], T. G. F. Li[7a], N. Liguori[18ab], M. Lorenzini[13a], V. Loriette[9b], G. Losurdo[13a], E. Majorana[3a], I. Maksimovic[9b], N. Man[10a], M. Mantovani[6ac], F. Marchesoni[12a], F. Marion[1], J. Marque[4], F. Martelli[13ab], A. Masserot[1], C. Michel[11], L. Milano[2ab], Y. Minenkov[16a], M. Mohan[4], N. Morgado[11], A. Morgia[16ab], B. Mours[1], L. Naticchioni[3ab], F. Nocera[4], G. Pagliaroli[16ac], L. Palladino[16ac], C. Palomba[3a], F. Paoletti[6a,4], M. Parisi[2ab], A. Pasqualetti[4], R. Passaquieti[6ab], D. Passuello[6a], G. Persichetti[2ab], F. Piergiovanni[13ab], M. Pietka[8d], L. Pinard[11], R. Poggiani[6ab], M. Prato[15], G. A. Prodi[18ab], M. Punturo[12a], P. Puppo[3a], D. S. Rabeling[7ab], I. Rácz[17], P. Rapagnani[3ab], V. Re[16ab], T. Regimbau[10a], F. Ricci[3ab], F. Robinet[9a], A. Rocchi[16a], L. Rolland[1], R. Romano[2ac], D. Rosińska[8cf], P. Ruggi[4], B. Sassolas[11], D. Sentenac[4], L. Sperandio[16ab], R. Sturani[13ab], B. Swinkels[4], M. Tacca[4], L. Taffarello[18c], A. Toncelli[6ab], M. Tonelli[6ab], O. Torre[6ac], E. Tournefier[1], F. Travasso[12ab], G. Vajente[6ab], J. F. J. van den Brand[7ab], C. Van Den Broeck[7a], S. van der Putten[7a], M. Vasuth[17], M. Vavoulidis[9a], G. Vedovato[18c], D. Verkindt[1], F. Vetrano[13ab], A. Viceré[13ab], J.-Y. Vinet[10a], S. Vitale[7a], H. Vocca[12a], R. L. Ward[5], M. Was[9a], K. Yamamoto[18bd], M. Yvert[1], A. Zadrożny[8e], J.-P. Zendri[18c]

[1] *Laboratoire d'Annecy-le-Vieux de Physique des Particules (LAPP), Université de Savoie, CNRS/IN2P3, F-74941 Annecy-Le-Vieux, France*

[2] *INFN, Sezione di Napoli[a]; Università di Napoli 'Federico II'[b] Complesso Universitario di Monte S.Angelo, I-80126 Napoli; Università di Salerno, Fisciano, I-84084 Salerno[c], Italy*

[3] *INFN, Sezione di Roma[a]; Università 'La Sapienza'[b], I-00185 Roma, Italy*

[4] *European Gravitational Observatory (EGO), I-56021 Cascina (PI), Italy*

[5] *Laboratoire AstroParticule et Cosmologie (APC) Université Paris Diderot, CNRS: IN2P3, CEA: DSM/IRFU, Observatoire de Paris, 10 rue A.Domon et L.Duquet, 75013 Paris - France*

[6] *INFN, Sezione di Pisa[a]; Università di Pisa[b]; I-56127 Pisa; Università di Siena, I-53100 Siena[c], Italy*

[7] *Nikhef, Science Park, Amsterdam, the Netherlands[a]; VU University Amsterdam, De Boelelaan 1081, 1081 HV Amsterdam, the Netherlands[b]*

[8] *IM-PAN 00-956 Warsaw[a]; Astronomical Observatory Warsaw University 00-478 Warsaw[b]; CAMK-PAN 00-716 Warsaw[c]; Bialystok University 15-424 Bialystok[d]; IPJ 05-400 Świerk-Otwock[e]; Institute of Astronomy 65-265 Zielona Góra[f], Poland*

[9] *LAL, Université Paris-Sud, IN2P3/CNRS, F-91898 Orsay[a]; ESPCI, CNRS, F-75005 Paris[b], France*

[10] *Université Nice-Sophia-Antipolis, CNRS, Observatoire de la Côte d'Azur, F-06304 Nice[a]; Institut de Physique de Rennes, CNRS, Université de Rennes 1, 35042 Rennes[b], France*

[11] *Laboratoire des Matériaux Avancés (LMA), IN2P3/CNRS, F-69622 Villeurbanne, Lyon, France*

[12] *INFN, Sezione di Perugia[a]; Università di Perugia[b], I-06123 Perugia, Italy*

[13] *INFN, Sezione di Firenze, I-50019 Sesto Fiorentino[a]; Università degli Studi di Urbino 'Carlo Bo', I-61029 Urbino[b], Italy*

[14] *Laboratoire Kastler Brossel, ENS, CNRS, UPMC, Université Pierre et Marie Curie, 4 Place Jussieu, F-75005 Paris, France*

[15] *INFN, Sezione di Genova; I-16146 Genova, Italy*

[16] *INFN, Sezione di Roma Tor Vergata[a]; Università di Roma Tor Vergata, I-00133 Roma[b]; Università dell'Aquila, I-67100 L'Aquila[c], Italy*

[17] *RMKI, H-1121 Budapest, Konkoly Thege Miklós út 29-33, Hungary*

[18] *INFN, Gruppo Collegato di Trento[a] and Università di Trento[b], I-38050 Povo, Trento, Italy; INFN, Sezione di Padova[c] and Università di Padova[d], I-35131 Padova, Italy*

The Virgo interferometer, a detector for gravitational waves located near Pisa in Italy, will soon be upgraded to become the next-generation detector Advanced Virgo. Advanced Virgo will be approximately ten times more sensitive than Virgo, with a design strain sensitivity better than $10^{-23}/\sqrt{\text{Hz}}$ near 100 Hz. This is expected to enable regular detections of gravitational waves and to yield significant astrophysical results. Many of the components of the detector will be changed for this upgrade. These changes include new core optics, a more powerful laser system, the signal-recycling technique, the use of homodyne detection at the output port, and an improvement of the vacuum system. The existing seismic isolation system in Virgo will be re-used. Advanced Virgo will form part of a global network of advanced gravitational wave detectors along with Advanced LIGO, GEO HF, and LCGT.

## 1 Introduction

Interferometric gravitational wave (GW) detectors of the first generation (Virgo[1], LIGO[2], GEO600[3]) have successfully completed their first long-duration data taking runs and are installing significant upgrades. Advanced Virgo is the project to upgrade the Virgo detector to a second generation instrument. Even though it will be hosted in the same infrastructures as Virgo, the Advanced Virgo sensitivity will be better by one order of magnitude over most of the detection band, and thus will increase by a factor of 1000 the accessible volume of the Universe when compared to initial Virgo. This paper provides a brief overview of the challenges that must be overcome to achieve this sensitivity increase, and the solutions designed to meet those challenges.

The Advanced Virgo detector will be based on the same basic principles of the Virgo detector, an electromagnetically coupled broadband gravitational wave antenna based on a Michelson interferometer with Fabry-Pérot cavities in the arms (cf. figure 1). The seismic isolation system

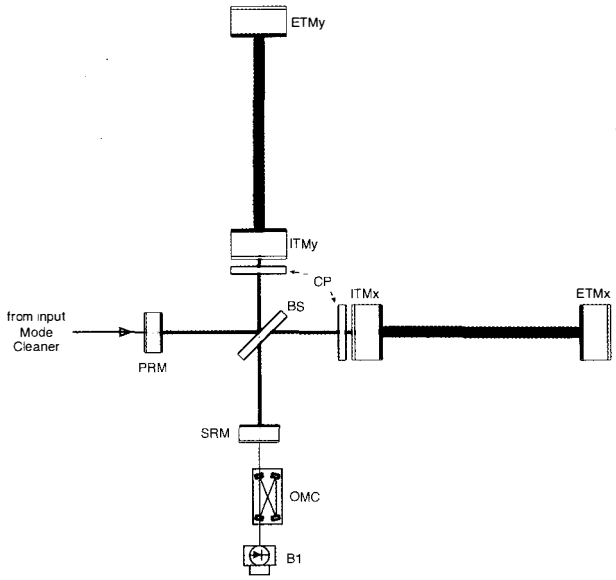


Figure 1: Optical layout of the Advanced Virgo interferometer. The input (ITM) and end (ETM) test mass mirrors are 42 kg and 35 cm in diameter. The beamsplitter (BS) is 55 cm in diameter. The interferometer has both power (PRM) and signal (SRM) recycling mirrors, the 3 km arm cavities are bi-concave, and thermal compensation plates (CP) are located between the ITMs and the BS.

(the superattenuator, cf. figure 2), will remain the same, as it already meets the requirements for Advanced Virgo[4].

Advanced Virgo will form part of a worldwide network of interferometric gravitational wave detectors, along with Advanced LIGO[5], LCGT[6], and GEO600[7], with all the detectors operating in coincidence, having comparable sensitivities, and co-operating on analysis of data. The expected event rate for the network for neutron star-neutron star inspiral and mergers will be around 40 events per year[8].

## 2 The path to Advanced Virgo

Figure 3 shows the expected (design) sensitivity curves of Virgo and Advanced Virgo, with contributions from several important noise sources. Each of the noise sources in Virgo that are larger than the designed Advanced Virgo sensitivity must be lowered, and we will briefly describe the technologies used to achieve this for each noise source.

## 3 Suspension thermal noise

At low frequencies (below 40 Hz) the Virgo sensitivity was limited by suspension thermal noise (shown in violet traces in figure 3), which arises from mechanical losses in the suspension wires[10]; the relationship between the mechanical losses and the thermal noise is given by the fluctuation-dissipation theorem. This noise will be reduced in Advanced Virgo by using so-called monolithic suspensions[11], where the optics are suspended by fused silica fibers rather than the steel wires used in Virgo. Much of the technology for these monolithic suspensions, including the pulling and bonding of the fused silica fibers, has already been demonstrated in Virgo+MS (Virgo+ with monolithic suspensions), an intermediate upgrade of the Virgo detector that is currently

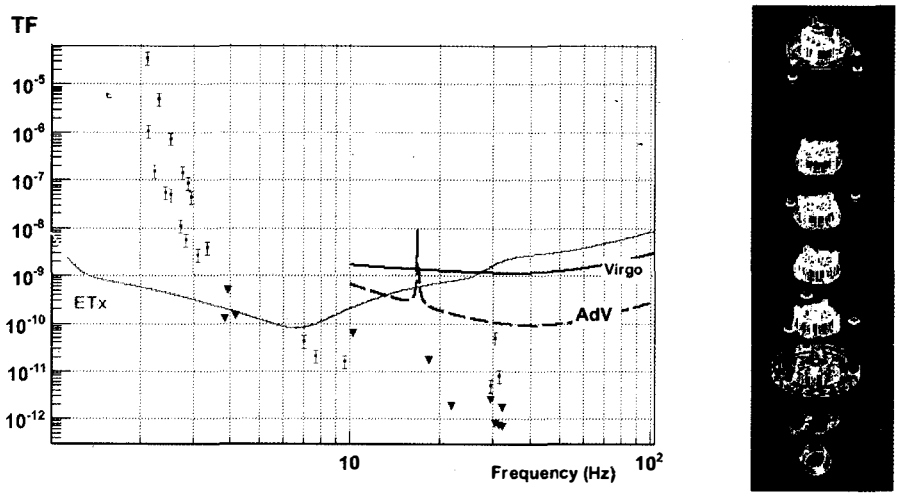


Figure 2: The superattenuator system employed in Virgo already meets the seismic isolation requirements for Advanced Virgo. On the left are measured upper limits on the seismic isolation transfer function of a superattenuator, shown with Virgo, Advanced Virgo, and Einstein Telescope[9] requirements. On the right is a rendering of a superattenuator.

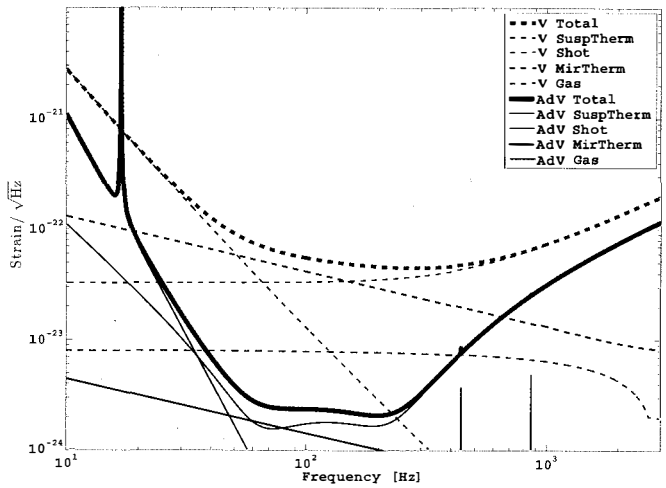


Figure 3: A comparison of the expected Virgo (dashed lines) and Advanced Virgo (solid lines) design sensitivities (in blue), shown as a strain-equivalent amplitude noise spectral density; contributions to the total noise from various specific noise sources are also shown . The noise contributions to the Virgo sensitivity which lie above the Advanced Virgo sensitivity are the principal targets of the upgrade technologies.

taking data with a modestly increased sensitivity compared to Virgo. The fibers themselves have an optimized geometry, with thick end points and a thinner middle section (approximately 300 $\mu$m in diameter), to minimize the thermal noise for a given maximum tensile load. Figure 4 shows a side view of a monolithic suspension from Virgo+MS, where the fiber thickness profile can be seen.

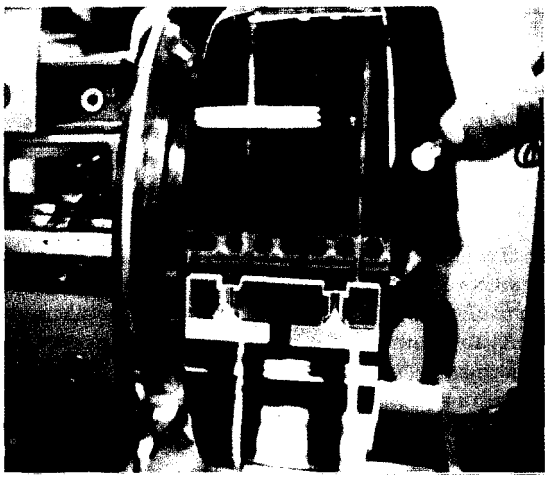

Figure 4: Side view of a monolithic suspension used in Virgo+MS. The pair of fused silica fibers used to suspend this mirror can be seen, along with the mechanism to attach the fibers to the test mass. In Advanced Virgo the test masses will be the same diameter (35 cm) but twice as thick: 20 cm instead of 10 cm.

The suspension thermal noise is also reduced by having heavier test masses, which for Advanced Virgo are 42 kg, twice as much as in Virgo and Virgo+MS. Further significant increases in this mass are limited by the weight carrying capacity of the superattenuator, which will remain unchanged.

For Advanced Virgo, the complete suspension design must be further upgraded to accommodate the thermal compensation plates (cf. figure 1 and section 5.1) which will be suspended from the same superattenuators as the input mirrors, while maintaining the superior thermal noise performance.

## 4 Mirror thermal noise

In the middle of the detection band, both Virgo and Advanced Virgo are limited by the mirror thermal noise (shown in black traces in figure 3) which arises due to thermal fluctuations of either the substrate or the multi-layer dielectric coating. Mirror thermal noise can be combatted with a combination of higher quality, lower loss materials for the mirror components, which directly reduces the thermal noise in the detection band, and with larger beam sizes, which average more of the fluctuating mirror surface and thus reduce their impact on the detector sensitivity. Both of these techniques will be used in Advanced Virgo, which will use lower loss materials and have larger beams than Virgo.

### *4.1 Beam size*

In Advanced Virgo the beam size on the arm cavity end mirrors (ETM) will be approximately 6 cm (radius to $1/e^2$ in intensity) and on the arm cavity input mirrors (and thus also the

beamsplitter) it will be approximately 5 cm. The beam waist size is less than 1 cm, located near the midpoint of the arm cavities. This is in contrast to Virgo, where the beam size on the end mirror was 5 cm and on the input mirror it was 2 cm, with the waist at the input mirror.

### *4.2 Substrate thermal noise*

Mechanical losses in the substrate material determine the quality factor of mechanical resonances, and this determines the level of broadband thermal noise arising from the substrate. Virgo was limited by thermal noise in the mirror substrates. For Advanced Virgo, a higher quality of fused silica with lower mechanical losses will be used for the test mass substrates, and thermal noise from the substrates should no longer be a limiting noise source.

### *4.3 Coating thermal noise*

The mechanical losses in the dielectric coating (alternating layers of silica and tantala) determine the quality factor of the mirror and as a consequence the displacement of the mirror surface due to its thermal vibration[12]. A research program has been undertaken at the *Laboratoire des Matériaux Avancés* (LMA) to improve the mechanical performances of these coatings without degrading the optical performances, by studying the properties of dielectric coatings composed of differing materials and constructed with varying recipes. Titanium doped $SiO_2/Ta_2O_5$ coatings developed at LMA are the best solution known so far[13], and are currently the baseline solution for Advanced Virgo.

## 5 Quantum noise

In laser interferometric gravitational wave detectors, only the quantum noise of the light (shot noise and radiation pressure noise, both of which arise from the particle nature of the laser light) is important, while the quantum noise of the masses is not significant. In Virgo, the only important quantum noise was the shot noise, which dominates above 200 Hz. In Advanced Virgo, which will operate with a signal recycling mirror, the distinction between shot noise and radiation pressure noise is not as clear, and so both are considered together as *quantum noise* (shown as red traces in figure 3).

### *5.1 Higher laser power*

At the higher frequencies of the detection band, where photon shot noise dominates, the shot noise limited signal to noise ratio scales inversely with the square root of the input laser power. To reduce this noise source, a higher power laser will be used (with 125W of 1064 nm laser light expected at the interferometer input, after the suspended input mode cleaning cavity). The reference solution to achieve such a high power is a master-oscillator power amplifier configuration, with a fiber-coupled NPRO as the master oscillator followed by two stages of fiber amplification from a commercial system.

The higher circulating laser power brings two complications: larger thermal effects from optical absorption, and the effects of optical rigidity.

#### Compensation of thermal effects

The foreseen level of injected power will increase the total circulating power to 700 kW in the arm cavities and about 5 kW in the power recycling cavity. Such high circulating powers mean that even with very low absorption optics, the heat absorbed by the mirrors and substrates will cause sufficient thermoelastic and thermorefractive changes to severely degrade the optical

performance of the interferometer. For this reason a thermal compensation system is necessary; this system illuminates the compensation plates (cf. figure 1) with a 10 $\mu$m laser projector with a pattern complementary to that of the heat deposited by the main laser beam. As 10 $\mu$m light is strongly absorbed by fused silica, much less power (about 15 W) is needed in this system than for the main laser light. In addition to this projector + compensation plate system, which compensates for thermorefractive effects in the mirror substrates, annular heating elements will surround the test masses to adjust the radii of curvature of these mirrors to counteract thermoelastic deformation of the mirror surfaces caused by absorption in the mirror coatings.

**Optical rigidity**

The high circulating power means that the dynamics of the interferometer mirrors, particularly in the arm cavities, are modified by the light fields due to radiation pressure. This results in opto-mechanical resonances (i.e., optical springs) in the differential length degree of freedom [14], which is the one sensitive to gravitational waves, and in the angular degrees of freedom[15]. Such opto-mechanical resonances are in general dynamically unstable, but appropriately designed control systems can quench these instabilities.

### *5.2 Signal recycling*

The use of the signal recycling technique permits a certain amount of flexibility in shaping the spectrum of quantum noise; this allows optimization of the sensitivity in the presence of other noise sources [14]. The sensitivity plotted in figure 3 has been optimized for neutron star binary inspirals, in the presence of suspension and mirror thermal noise. Small changes in the parameters of the signal recycling cavity (such as a small change in the reflectivity of the signal recycling mirror or even a microscopic, sub-wavelength adjustment of the signal recycling mirror position) can modify the quantum noise, to maximize the sensitivity to another source (e.g., a particular millisecond pulsar, or stellar mass black hole binaries).

### *5.3 DC readout*

In place of the optical heterodyne technique used in Virgo, Advanced Virgo will use optical homodyne detection in the form of the technique known as DC readout. This technique involves a slight detuning of the differential arm degree of freedom (the one which is also sensitive to gravitational waves) slightly from destructive interference to allow a small amount of light to leak out the detection port to serve as a local oscillator. Because this light has been stored in the interferometer, it has been passively filtered by the so-called coupled-cavity pole[16]. This passive optical filtering, combined with the laser pre-stabilization system, means this light is a very low noise optical local oscillator in the detection band. Furthermore, optical homodyne detection has a lower level of shot noise than optical heterodyne detection[17]. To implement DC readout an output mode cleaner (OMC in figure 1) is placed after the interferometer and before the photodetector (B1 in figure 1).

### *5.4 Optical losses*

The surface quality of the test mass substrates is an important factor in the optical performance (i.e., the optical losses) of the interferometer, which can impact the quantum noise limited sensitivity. To achieve an appropriately low level of surface figure error, a corrective coating process has been developed at LMA. This process is expected to suppress surface figure errors with spatial scale larger than $50\,\mathrm{m}^{-1}$, which have a large effect on the optical performance of km-scale cavities with large beam sizes. The apparatus for this corrective coating has been

constructed, and the first tests of this process on large scale mirrors (i.e., the 35 cm diameter of the Advanced Virgo substrates) will take place soon.

## 6 Residual gas noise

Residual gas in the 3 km beam tubes can induce phase fluctuations in the laser light circulating in the Fabry-Pérot arm cavities, resulting in noise in the interferometer output (the green traces in figure 3). The current Virgo vacuum system operates at a residual pressure of about $10^{-7}$ mbar; this level must be reduced to about $10^{-9}$ mbar to meet the Advanced Virgo requirements. This will be done by performing a vacuum bake-out of the beam tubes and installing cryotraps at each end of each beam tube. The cryotraps will allow regular intervention into the vacuum system at the mirror locations without spoiling the level of vacuum in the beam tubes through water migration.

## 7 Conclusions

Achieving a factor of 10 sensitivity improvement over Virgo requires pushing the limits of technology on several frontiers. The maturing Advanced Virgo design will meet these limits. Expected to be online in 2015, Advanced Virgo will be a crucial part of the network of next generation gravitational wave detectors that will usher in the era of gravitational wave astronomy.


## Acknowledgments

Advanced Virgo is a joint project of the *Centre National de la Recherche Scientifique* (CNRS) and the *Istituto Nazionale di Fisica Nucleare* (INFN).


## References


1. F. Acernese et al., *Class. Quant. Grav.* **25**, 184001 (2008)
2. B. Abbott, et al., *Rep. Prog. Phys.* **72**, 076901 (2009)
3. H Grote and the LIGO Scientific Collaboration, *Class. Quant. Grav.* **27**, 084003 (2010)
4. F. Acernese et al., *Astropart. Phys.*, **33**, 182 (2010)
5. G. Harry and the LIGO Scientific Collaboration *Class. Quant. Grav.* **27**, 084007 (2010)
6. K. Kuroda (on behalf of the LCGT Collaboration), *Class. Quant. Grav.* **27**, 084004 (2010)
7. B. Willke et al., *Class. Quant. Grav.* **23**, S207 (2006)
8. J. Abadie et al., *Class. Quant. Grav.* **27**, 173001 (2010)
9. M. Punturo et al., *Class. Quant. Grav.* **27**, 194002 (2010)
10. P.R. Saulson. *Phys. Rev.* D **42**, 2437 (1990)
11. M. Lorenzini and the Virgo Collaboration, *Class. Quant. Grav.* **27**, 084021 (2010)
12. G.M. Harry, *et al.*, *Appl. Opt.*, **45**, 1569 (2006)
13. C.Comtet *et al.*, *Proceedings of the 42nd Rencontres de Moriond*, (2007)
14. A. Buonanno and Y. Chen, *Phys. Rev.* D **64**, 042006 (2001)
15. J.A. Sidles and D.Sigg. *Physics Letters A*, **354**, 167 172, (2006).
16. J.B. Camp, *et al.*, *J. Opt. Soc. Am. A*, **17** 12 (2000)
17. A.Buonanno, Y.Chen, and N.Mavalvala. *Phys. Rev.* D **67**, 122005 (2003)